DOI: 10.1002/cbic.200800089

Covalent Fluorescence Labeling of His-Tagged Proteins on the Surface of Living Cells

Martin Hintersteiner,[a] Thomas Weidemann,[b] Thierry Kimmerlin,[a] Nimet Filiz,[a] Christof Buehler,[a] and Manfred Auer*[a]

Mechanistic studies in living cells require fluorescent labeling of the proteins of interest. The widespread application of GFP variants in combination with fluorescence microscopy has had an immense impact on our understanding of the dynamic processes in living cells. Due to the recent progress in detection technologies and microspectroscopy, the expansion of the available labeling strategies to more photostable, smaller, multicolor reagents has become an active field of research.[1–6] The majority of these new fluorescent tags are small chemical entities that bind with various affinities to genetically fused peptide stretches in the protein of interest.[7–14] Confocal images provide snapshots of dynamic molecular rearrangements. However, the observation of such processes by medium to high-affinity fluorescent ligands can be complicated because of a floating background inherent to the limited stability of the complex. Thus, covalent, site-selective protein-labeling techniques offer improvements in separating cellular from tag-specific biochemical events. Up to now much emphasis has been given to covalent-labeling strategies that rely on enzymatic couplings;[15–19] only recently has a novel nonenzymatic protein-labeling concept been described.[20]

Herein we present an alternative strategy that combines the reversible binding of a medium affinity probe with a photoreactive moiety to generate a covalent linkage in the proximity of the tag. Substituted arylazides have been widely used in protein-interaction studies for photoaffinity labeling.[21,22] Photoactivation is well suited for generating covalent bonds because of the simplicity of the activation procedure, good efficiencies, and short timescales of the reaction.[23,24] The combination of a photocrosslinking moiety and an oligohistidine directing Ni-NTA group has previously been exploited for in vitro protein functionalization to build self-assembling protein arrays.[25] Reasoning that this method could provide a simple means of covalently tagging proteins on living cells, we synthesized a trifunctional labeling tag that consists of a fluorophore, a Ni-NTA moiety, and a photoactivatable arylazide. Our labeling strategy comprises two steps: reversible binding at the His-tag of a target protein followed by irreversible photolinkage at the binding site (Figure 1). Irreversible crosslinking to a recombinant His-tagged GFP was demonstrated in vitro by fluorescence spectroscopy and quantitative SDS-PAGE. As the main proof of concept of the new tagging technology for microspectroscopy, a His-tagged chain of a single pass transmembrane receptor was covalently labeled and quantitatively characterized on a living cell.

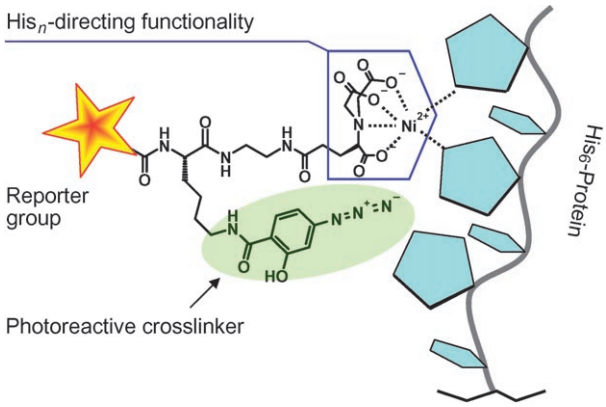

Figure 1. The principle of an irreversible NTA probe for labeling of His-tagged proteins in vitro and in living cells is based on the combination of a histidine directing NTA functionality with an activatable (photo-)crosslinker. The mono-NTA group reversibly binds to the oligohistidine-tagged protein and introduces specificity into the otherwise unspecific crosslinking reaction. The ideal crosslinker should be of moderate reactivity to avoid nonspecific labeling. It must be sufficiently reactive to achieve high levels of labeled product. In addition, a suitable tripodal backbone has to be chosen for linking the NTA and crosslinker moiety to a fluorophore and for appropriate positioning of the three elements.

The synthesis of trifunctional His-directed labeling probes started from the previously described *tert*-butyl protected NTA **1**[8] (Scheme 1). Amidation with benzylethane-1,2-diamine was followed by the introduction of an orthogonally protected lysine (Boc-Lys(*Z*)-OH) as flexible branching point. After hydrogenolytic Z-deprotection, the hydroxy-arylazide crosslinker (ASA) was coupled to the ε-amino group of the lysine backbone, using succinimidyl activated ester. Subsequently the *tert*-butyl and *tert*-butoxy protecting groups were removed with trifluoroacetic acid (TFA) and the fluorescent dye TMR or the quencher QSY7 was coupled to the remaining α-amino group. Finally, complexation of the mono-NTA moiety with Ni^{2+} and purification by preparative HPLC yielded probes NTA-ASA-TMR **5** and NTA-ASA-QSY7 **6**.

First the binding and fluorescence properties of compounds **5** and **6** were investigated by conventional fluorescence spec-

[a] *Dr. M. Hintersteiner,[+] Dr. T. Kimmerlin,[+] N. Filiz, Dr. C. Buehler, Dr. M. Auer*
Novartis Institutes for BioMedical Research (NIBR)
Innovative Screening Technologies
Brunnerstrasse 59, 1235 Vienna (Austria)
Fax: (+43) 1-86634-593
E-mail: manfred.auer@novartis.com

[b] *Dr. T. Weidemann[+]*
Max Planck Institute of Molecular Cell Biology and Genetics
Pfotenhauerstrasse 108, 01307 Dresden (Germany)

[+] *These authors contributed equally to this work.*

Supporting information for this article is available on the WWW under http://www.chembiochem.org or from the author.

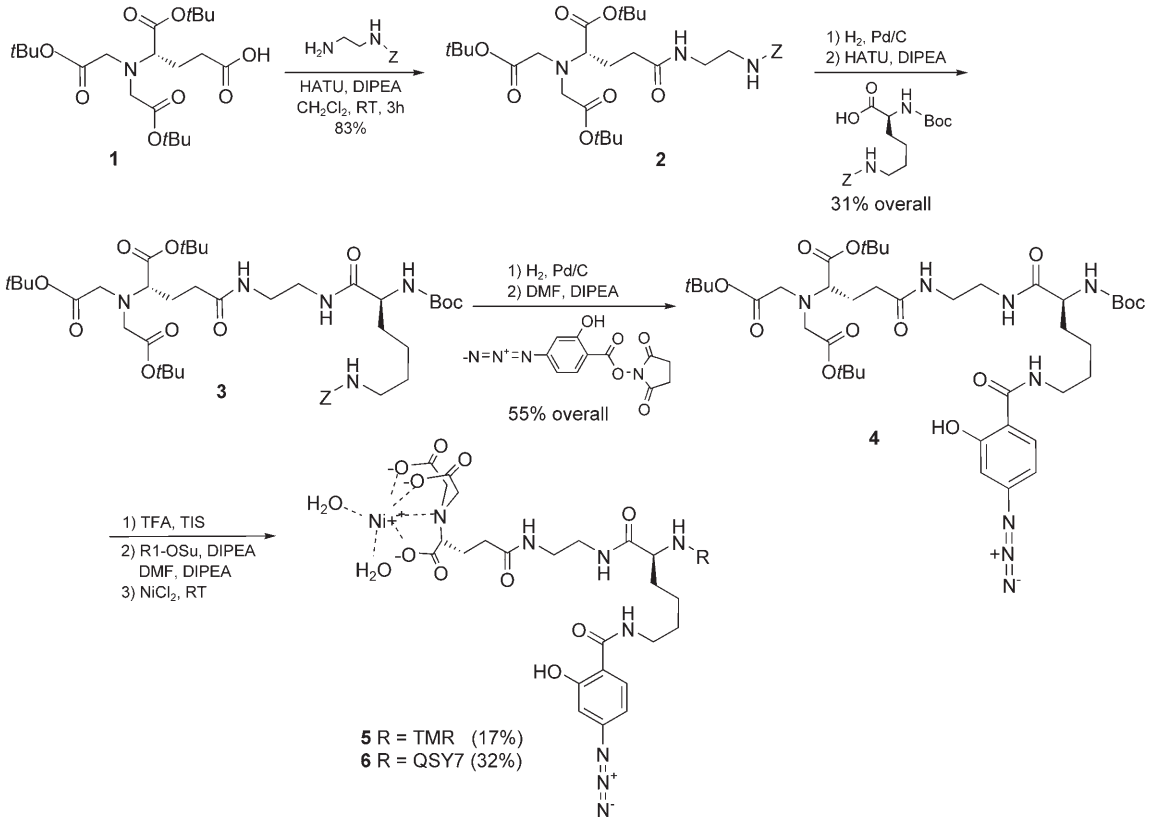

Scheme 1. The synthesis of the irreversible NTA-ASA probes **5** and **6** starts from the commercially available *tert*-butyl-protected amino acid **1**. Conjugation of educt **1** to *Z*-protected diaminoethane yielded the elongated fully protected NTA **2**. Compound **3** was obtained after hydrogenolytic deprotection of the elongated NTA and coupling to Boc-Lys(*Z*)-OH. Again, hydrogenolytic deprotection and coupling of the resulting intermediate to ASA-SE afforded the key intermediate Boc-NTA-ASA **4**. Deprotection of all protecting groups on compound **4** with TFA and conjugation to TMR or QSY7 yielded the final irreversible NTA-ASA probes **5** and **6**, respectively.

troscopy. We used a FRET-based assay system, as described by Guignet et al.[7] A purified recombinant GFP with a C-terminal His-tag, GFP-C-His, served as a FRET donor for NTA-ASA-TMR **5** or NTA-ASA-QSY7 **6**, the acceptors. Quenching of the donor because of energy transfer directly reflects the fraction of complexed GFP-C-His (Figure 2A). The affinity was determined by measuring the degree of donor quenching under equilibrium conditions for increasing ligand concentrations (Figure 2C). NTA-ASA-TMR **5** showed an equilibrium dissociation constant of $K_d = 1 \pm 0.07$ μM. For comparison, the K_d values of previously described compounds NTA-I and NTA-II were also determined (see the Supporting Information). Without photoactivation, binding of probes **5** and **6** to oligohistidine-tagged proteins is reversible and mediated by a d^8 coordinated Ni^{2+}. Thus, ethylenediaminetetraacetate (EDTA), added in excess (>250-fold), competes for free Ni^{2+} ions, and binding is successively reversed. The time course of this competition reaction critically depended on the substituents of the NTA. For example, unquenching was complete for NTA-I after 5 min, for NTA-ASA-TMR **5** after 10 min, and the release of NTA-ASA-QSY7 **6** took more than 1 h under similar conditions (Figure 2B). The amount of fluorescence recovered by EDTA was about 90% for NTA-I, whereas for the NTA-ASA derivatives only 60–70% was recovered. The data suggest that a large excess of NTA-ASA probes **5** and **6** versus GFP-C-His in this assay (1000-fold) promotes residual His-tag-independent binding. In contrast to dissociation, binding of the compounds is completed within several seconds. To finally demonstrate the covalent linkage, we included a photoactivation step between binding and EDTA mediated release of the NTA-ASA probes **5** and **6**. As expected, the UV-irradiated samples showed only 10% EDTA-mediated fluorescence recovery as compared to nonirradiated controls (Figure 2A). It is noteworthy that photoactivation (120 mJ) of NTA-ASA-TMR **5** in the absence of protein reduces the fluorescence to about 55%, whereas free TMR-COOH control showed no bleaching. We therefore assume that the activated arylazide might, to a certain extent, self-react and thereby destroy the integrity of the conjugated π-system. Moreover, the molecular brightness of Ni^{2+} complexed NTA-ASA-TMR **5** at 543 nm excitation was determined by confocal fluorescence correlation spectroscopy and compared to the molecular brightness of the free dye TMR-COOH in phosphate-buffered saline (PBS; Table S1). The data indicate a moderate quenching effect of Ni^{2+} on the fluorescence emission of TMR, resulting in a 30% decrease in molecular brightness, as compared to the unconjugated dye.

To prove that photoactivation establishes a stable covalent linkage, SDS-PAGE was used to remove nonconjugated NTA-ASA **5** under harsh conditions. GFP-C-His (1.25 μM) was incubated with a fourfold excess of NTA-ASA-TMR **5**, photoactivat-

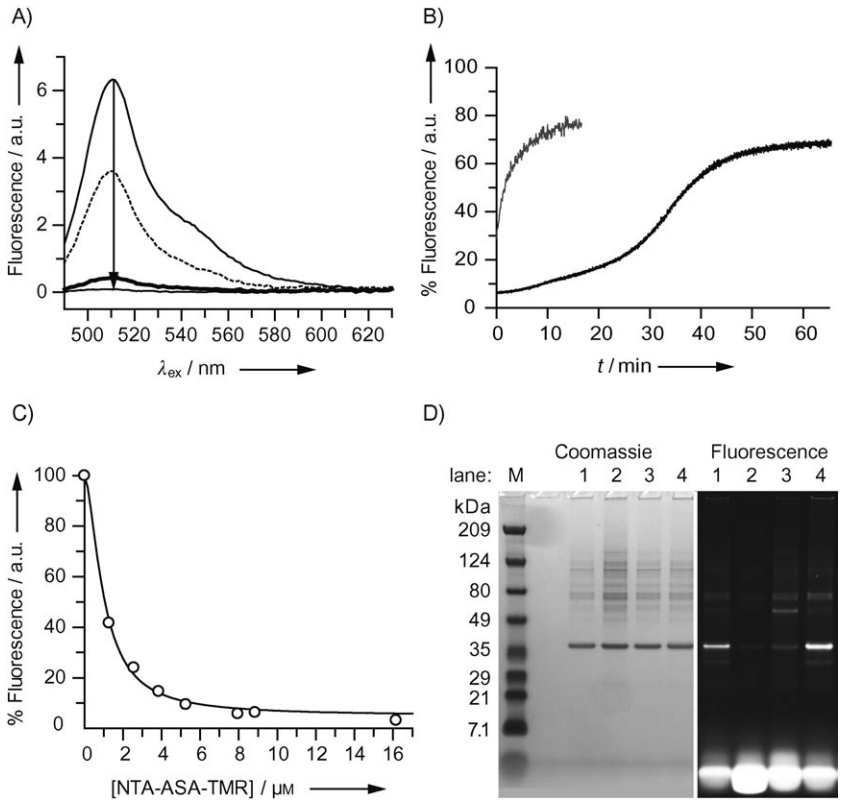

Figure 2. Covalent crosslinking of NTA-ASA derivatives in solution. A) The emitted GFP-C-His fluorescence (15 nM, straight) is quenched by addition of nonfluorescent NTA-ASA-QSY7 **6** (10 μM, red) due to FRET (arrow). Competing for Ni^{2+} with a 250-fold excess of EDTA after crosslinking (120 μJ) leads to a recovery of residual 10% of the donor fluorescence (green) with respect to a nonirradiated control (dotted). B) Kinetics of EDTA unquenching for NTA-ASA-TMR **5** (black) and -QSY7 **6** (gray) under similar conditions. C) Determination of the equilibrium dissociation constant for NTA-ASA-TMR **5** by applying the Hill equation.[5] D) SDS-PAGE of GFP-C-His (1.25 μM) incubated with NTA-ASA-TMR (5 μM). The reaction was crosslinked with 120 mJ (lanes 1 and 3), 0 mJ (lane 2), or 240 mJ (lane 4). Covalent linkage in lane 3 was prevented by a 100-fold excess of EDTA (0.5 μM).

ed under several conditions and loaded on the gel (Figure 2D). The gel clearly shows that fluorescent compound **5** associates with the GFP band. A nonactivated control and an EDTA quenched sample showed only weak fluorescence. Bound and free compound was quantified by digital image analysis. The fractional intensities associated with the GFP-band versus free dye is 9% for a dosage of 120 mJ and 15% for 240 mJ. Further increase of the dosage had no effect. Neglecting the small background of protein impurities running at higher molecular weights we recalculated these values with respect to the fraction of bound ligand, which resulted in a crosslink efficiency of 45% (120 mJ) and 75% (240 mJ) at the binding site.

To test covalent His-tag mediated labeling of extracellular parts of membrane receptors via NTA-ASA-TMR at the cellular surface, we transiently expressed a His-tagged interleukin-4 receptor (IL4R) in human embryonic kidney cells (HEK 293 T). The receptor construct (NHis-IL4Rac-GFP) comprises a hexahistidine stretch at the N terminus followed by the extracellular and transmembrane domains of the interleukin-4 receptor α chain. The cytoplasmic tail of the receptor was replaced by eGFP. In this configuration, the His-tag is expressed extracellularly, whereas the GFP is located in the cytosol. The double-tagged receptors allow estimation of crosslinking efficiencies provided that receptor and ligand densities are observed in orthogonal color channels.

For labeling, the cells were washed, incubated with NTA-ASA-TMR **5** (0.5–2.6 μM in PBS^{++}), UV-irradiated for 40 s applying 120 mJ, and washed several times with culture medium. Figure 3A–F illustrates confocal images of a transfected cell in a layer of nontransfected neighbors. In the GFP-channel only the transfected cell is visible. The fluorescent receptors are clearly localized in the membrane. Typical for high expression levels, the unprocessed receptors accumulate in intracellular membrane systems. The TMR color channel nicely shows that staining of transfected cells with NTA-ASA-TMR **5** is restricted to the surface membrane suggesting that the compound is not cell penetrating without any specific additives such as DMSO. Cells expressing a control vector lacking the His-tag, IL4Rac-eGFP, did not accumulate TMR-fluorescence over background (Figure 3G–I).

In order to assess cellular labeling quantitatively, we calibrated the confocal images with a previously described method.[26] In brief, we determined the molecular brightness of eGFP and NTA-ASA-TMR with fluorescence correlation spectroscopy (FCS) in the same optical setup as used for confocal imaging. With the numbers obtained by FCS, the pixel intensities were converted into particle concentrations. From the concentration maps, average values for eGFP and NTA-ASA-TMR **5** in the surface membrane were extracted with a script (MatLab). According to Table 1, the transfected cells express lower micromolar concentrations of receptor. A cross-comparison with the intensities detected in imaging in the TMR channel shows that 10.4%, 0.56 μM (cell 1) and 4.2%, 0.51 μM (cell 2) of the receptors were labeled (using a confocal volume of 0.25 fL in cellular microspectroscopy, a concentration of 1 μM equals ~3500 molecules per μm^2; at the cell surface). Surface intensity measurements of the neighboring nontransfected cells showed a not negligible background staining reflecting a particle concentration of 100–110 nM. In both cells which were chosen for quantitative image analysis, a signal-to-noise ratio (S/N) of 5 was achieved. Assuming a one-to-one binding model with a K_d of 1 μM for NTA-ASA-TMR complexation with the IL4-R α chain His-tag, we calculated the fraction of complexed receptor under equilibrium conditions to be 9.2% and 4.6% for the re-

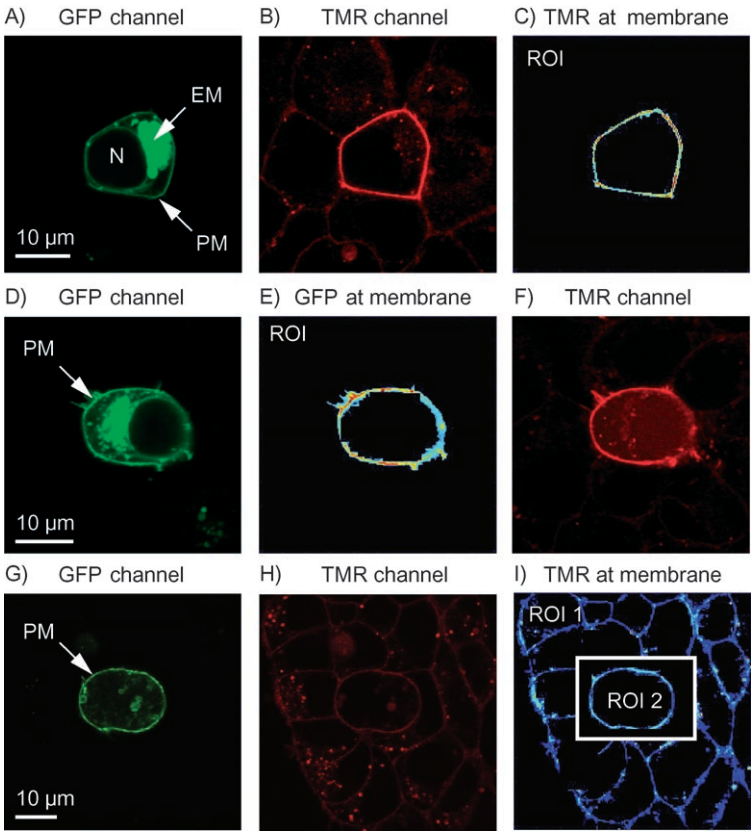

Figure 3. Covalent crosslinking of NTA-ASA-TMR to a His-tagged receptor chain at the cell surface. A)–C) and D)–F) two cells expressing NHis-IL4Rac-GFP, G)–I) a cell expressing IL4Rac-GFP as a negative control. Confocal cross sections in the GFP-channel (A, D, G) show that the receptors are expressed in endogenous membrane systems (EM) associated with the nucleus (N) as well as at the surface plasma membrane (PM). After crosslinking, NTA-ASA-TMR is found at the plasma membrane of His-tag expressing cells (B, F) but not for a negative control of similar expression level (H, compare concentration values in Table 1). The plasma membrane was selected as a region of interest (ROI), examples shown for the TMR- (C, I) and the GFP-channel (E) of the three cells, respectively. Panel I) illustrates how the membranes of neighboring nontransfected cells (ROI 1) were discriminated from the membrane of a receptor expressing cell (ROI 2) in order to generate the values in Table 1.

Table 1. Quantification of cellular labeling.

Cell #	NHis-IL4Rac-eGFP [µM][a]	NTA-ASA-TMR [µM][b]	NTA-ASA-TMR [µM][c]	S/N[d]
1[e]	4.3	0.56	0.11	5.0
2[e]	9.8	0.51	0.10	5.2
3[f]	6.6	0.58	0.48	1.2

[a] With a confocal volume of 0.25 fL, a concentration of 1 µM equals ~3500 molecules per μm^2, detected in the cell membrane; [b] on the surface of transfected cells; [c] on the surface of nontransfected cells; [d] signal-to-noise ratio; [e] Incubation with 0.5 µM NTA-ASA-TMR; [f] Incubation with 2.6 µM NTA-ASA-TMR.

ceptor concentrations determined at the cell surface of cells 1 and 2, respectively. These values are in remarkable agreement with the complex concentrations determined from the images after covalent crosslinking. To conclude, receptor labeling with our covalent TMR labeling tags reached a significant S/N level on cells expressing micromolar concentrations of His-tagged receptor. Lower surface expression did not accumulate surface staining above background.

In summary, NTA-ASA derivatives **5** and **6** represent a new class of probes for site-specific covalent labeling of His-tagged proteins. We show that the labeling strategy can be successfully applied to living cells. The medium affinity of the Ni-NTA complex allows the removal of unreacted reagent. Moreover, the labeling procedure is simple and fast. Further efforts should find optimized combinations of the fluorescent dye used in combination with different photocrosslinker moieties. A reduced hydrophobicity of the probes or the use of decahistidine tags might significantly improve the selectivity and sensitivity of the method. We note that the concept of combining a photoreactive probe with a medium affinity site-directing functionality is not restricted to the NTA/oligohistidine system.

Acknowledgements

We thank Rainer Siedler for help in optical alignment, Marion Kala for editorial work, and Rene Amstutz for continued support of this project.

Keywords: confocal · fluorescence imaging · IL-4R · Ni-NTA · photoaffinity labeling

[1] J. A. Prescher, C. R. Bertozzi, *Nat. Chem. Biol.* **2005**, *1*, 13–21.
[2] I. Chen, A. Y. Ting, *Curr. Opin. Biotechnol.* **2005**, *16*, 35–40.
[3] K. M. Marks, G. P. Nolan, *Nat. Methods* **2006**, *3*, 591–596.
[4] J. H. van Maarseveen, J. N. H. Reek, J. W. Back, *Angew. Chem.* **2006**, *118*, 1873–1875; *Angew. Chem. Int. Ed.* **2006**, *45*, 1841–1843.
[5] T. L. Foley, M. D. Burkart, *Curr. Opin. Chem. Biol.* **2007**, *11*, 12–19.
[6] I. S. Carrico, B. L. Carlson, C. R. Bertozzi, *Nat. Chem. Biol.* **2007**, *3*, 321–322.
[7] E. G. Guignet, R. Hovius, H. Vogel, *Nat. Biotechnol.* **2004**, *22*, 440–444.
[8] S. Lata, A. Reichel, R. Brock, R. Tampe, J. Piehler, *J. Am. Chem. Soc.* **2005**, *127*, 10205–10215.
[9] S. Lata, M. Gavutis, R. Tampe, J. Piehler, *J. Am. Chem. Soc.* **2006**, *128*, 2365–2372.
[10] S. R. Adams, R. E. Campbell, L. A. Gross, B. R. Martin, G. K. Walkup, Y. Yao, J. Llopis, R. Y. Tsien, *J. Am. Chem. Soc.* **2002**, *124*, 6063–6076.
[11] B. R. Martin, B. N. Giepmans, S. R. Adams, R. Y. Tsien, *Nat. Biotechnol.* **2005**, *23*, 1308–1314.
[12] A. Ojida, K. Honda, D. Shinmi, S. Kiyonaka, Y. Mori, I. Hamachi, *J. Am. Chem. Soc.* **2006**, *128*, 10452–10459.
[13] C. T. Hauser, R. Y. Tsien, *Proc. Natl. Acad. Sci. USA* **2007**, *104*, 3693–3697.
[14] B. Krishnan, A. Szymanska, L. M. Gierasch, *Chem. Biol. Drug Des.* **2007**, *69*, 31–40.
[15] J. L. Meier, A. C. Mercer, H. Rivera, Jr., M. D. Burkart, *J. Am. Chem. Soc.* **2006**, *128*, 12174–12184.
[16] A. Keppler, S. Gendreizig, T. Gronemeyer, H. Pick, H. Vogel, K. Johnsson, *Nat. Biotechnol.* **2003**, *21*, 86–89.
[17] A. Keppler, H. Pick, C. Arrivoli, H. Vogel, K. Johnsson, *Proc. Natl. Acad. Sci. USA* **2004**, *101*, 9955–9959.
[18] I. Chen, M. Howarth, W. Y. Lin, A. Y. Ting, *Nat. Methods* **2005**, *2*, 99–104.
[19] M. Howarth, K. Takao, Y. Hayashi, A. Y. Ting, *Proc. Natl. Acad. Sci. USA* **2005**, *102*, 7583–7588.

[20] H. Nonaka, S. Tsukiji, A. Ojida, I. Hamachi, *J. Am. Chem. Soc.* **2007**, *129*, 15777–15779.
[21] M. Suchanek, A. Radzikowska, C. Thiele, *Nat. Methods* **2005**, *2*, 261–267.
[22] G. Dorman, *Top. Curr. Chem.* **2001**, *211*, 169–225.
[23] Y. Hatanaka, Y. Kanaoka, *Heterocycles* **1998**, *47*, 625–632.
[24] F. Kotzyba-Hibert, I. Kapfer, M. Goeldner, *Angew. Chem.* **1995**, *107*, 1391–1408; *Angew. Chem. Int. Ed. Engl.* **1995**, *34*, 1296–1312.
[25] G. D. Meredith, H. Y. Wu, N. L. Allbritton, *Bioconjugate Chem.* **2004**, *15*, 969–982.
[26] T. Weidemann, M. Wachsmuth, T. A. Knoch, G. Muller, W. Waldeck, J. Langowski, *J. Mol. Biol.* **2003**, *334*, 229–240.

Received: February 8, 2008
Published online on May 6, 2008

